

ORIGINAL RESEARCH ARTICLES

EXPRESSION OF PHOSPHATE TRANSPORTERS IN OPTIMIZED CELL CULTURE MODELS FOR DENTAL CELLS BIOMINERALIZATION

Laure Merametdjian^{1,2,3}, Amandine David^{1,2}, Nina Bon^{1,2}, Greig Couasnay^{1,2}, Jérôme Guicheux^{1,2,3}, Céline Gaucher^{4,5}, Sarah Beck-Cormier^{1,2} and Laurent Beck^{1,2*}

¹ INSERM, U791, LIOAD, Nantes, F-44042, France. ² Université de Nantes, UFR Odontologie, UMR_S 791, Nantes, F-44042, France. ³ CHU Nantes, PHU 4 OTONN, Nantes, F-44042, France. ⁴ Dental School University Paris Descartes PRES Sorbonne Paris Cité, EA 2496, Montrouge, F-92120, France ⁵ AP-HP, Odontology Department, Hôpital Albert Chenevier, GHM, AP-HP, Créteil, F-94010, France
* Corresponding author: Laurent Beck, Ph.D. INSERM U791-LIOAD, Faculté de Chirurgie Dentaire 1, place Alexis Ricordeau, 44042 Nantes cedex 1, France, email: laurent.beck@inserm.fr

Abstract / Résumé

Phosphate is a key component of dental mineral composition. The physiological role of membrane proteins of dental cells is suspected to be crucial for mineralization mechanisms. Contrary to published data related to calcium, data on regulation of phosphate flux through membrane of mineralizing cells are scarce. To address this lack of data, we studied the expression of six membranous phosphate transporters in two dental cell lines: a rat odontoblastic cell line (M2H4) and a mouse ameloblastic cell line (ALC) for which we optimized the mineralizing culture conditions. La place essentielle du phosphate dans la composante minérale de la dent laisse supposer un rôle physiologique déterminant pour les protéines membranaires permettant son entrée dans les cellules dentaires. Contrairement à celles disponibles pour le calcium, les données sur les molécules permettant la production et la régulation du flux de phosphate aux sites de formation du minéral par les cellules minéralisantes de la dent sont peu connues. Nous avons analysé dans cette étude six transporteurs de phosphate membranaires dans deux lignées cellulaires dentaires: une lignée d'odontoblastes de rat (M2H4) et une lignée améloblastique murine, les ALC, pour laquelle nous avons optimisé les conditions de culture minéralisantes.

Keywords

phosphate, mineralization, ALC, M2H4

Introduction

The tooth is the most mineralized organ of the body and is composed of both calcified tissues like dentin and cementum, and mineral acellular structures like enamel. For each dental structure, the mineralization process has specific features. Whereas enamel mineralization requires specific proteins such as amelogenins or enamelin, dentin mineralization mechanisms are closer to those taking place in bone by involving collagenous and non-collagenous matrix proteins. In addition, dentin mineralization shows significant differences, between the outer mantle and the circumpulpal dentin in term of mineral density, and also between the intertubular and peritubular areas in term of protein's matrix composition (Goldberg et al., 2011). Cementum also displays its own specificities with some distinguishable cellular/non cellular and fibrillar/non fibrillar areas along the roots (Goncalves et al., 2005).

Two main mineral deposition mechanisms are reported in the literature, namely, matrix vesicles budding from mineralizing cells, or secretion of a non-mineralized extracellular matrix that will eventually become a mineralized structure in supersaturated calcium

(Ca)-phosphate (Pi) environment in which mineral will nucleate (Veis et al., 2013). These mechanisms have been mainly described in bone, and the mineralization processes involved in dentin and enamel are much less known. Nonetheless, the mineral part of any mineralized tissue consists of Pi and Ca ions that will accumulate, be combined together and stabilized in the form of hydroxyapatite ($\text{Ca}_{10}(\text{PO}_4)_6(\text{OH})_2$), eventually combined with minor ions giving rise to biological apatites. The essential requirement of Ca and Pi for tooth mineralization raises the question of the mechanisms underlying the production and regulation of ions fluxes at the mineral formation sites of the tooth. Whereas Ca transport and regulation in the dental enamel have been partially described (Hubbard M.J., 2000), Pi transport on the dental mineralization sites is still a large question mark.

In mammals, there are six identified Na-Pi cotransporters located at the plasma membrane and responsible for Pi entry into the cell. These transporters have been historically separated into three families, based on their sequence similarities and tissue expression. The first family, NPT1/SLC17A1, is expressed mostly in kidney and liver, but also in the brain. Although NPT1 displays a Pi transport activity in cultured cells *in vitro*, its physiological function is now known as being a chloride-dependent urate exporter (Iharada et al., 2010). The second SLC34 family comprises three members, among which Npt2a/SLC34A1 and Npt2c/SLC34A3 are primarily expressed in the proximal tubule of the kidney, whereas Npt2b/SLC34A2 has a wider expression (mainly lung and intestine) (Wagner et al., 2014). The third family is represented by PiT1/SLC20A1 and PiT2/SLC20A2, which are expressed in a large number of tissues (Forster et al., 2013).

In recent years, considerable progress has been made in determining the physiological function of these transporters. By generating the first knockout mouse model for a Pi transporter, we have shown that Npt2a is the main carrier responsible for the reabsorption of Pi by the kidney (Beck et al., 1998), at least in rodents. More recent studies have confirmed these data and in addition, showed that the function of Npt2c carrier, expressed in the same segments of the nephron than Npt2a, was to increase the reabsorption capacity of Pi during growth. However, the physiological role of Npt2c in rodents remains minor, since

its deletion did not aggravate the phenotype of the Npt2a knockout mice (Miyamoto et al., 2011). In both models, although the dental phenotype has not been explored in details, the animals showed no major eruption failure or dental mineralization defects (L. Beck, unpublished data). Invalidation of the Npt2b gene in mice is embryonic lethal at E10.5 (Shibasaki Y., BBRC 2009). A tissue-specific inactivation in the intestine was performed, revealing its essential role in the intestinal absorption of Pi (Sabbagh et al., 2009). When mutated in humans, loss of Npt2b results in lung and testis calcifications (Corut et al., 2006). Its role in tooth mineralization *in vivo* has not been formally demonstrated. However, some studies have shown that Npt2b was expressed in odontoblasts and that its expression correlated with that of the Phex gene (Onishi et al., 2007). Interestingly, mutations of Phex in humans cause osteomalacia, impaired renal reabsorption of Pi, together with an abnormal mineralization of cementum and dentin (Gaucher et al., 2009). Similarly to SLC17 and SLC34 transporters, the involvement of PiT1 and PiT2 in dental mineralization is poorly described. The inactivation of the PiT1 gene in mice leads to a lethal phenotype at mid gestation, and does not allow to study its physiological role in the tooth (Beck et al., 2010). Although, the transgenic cover expression of PiT1 in rats has suggested the involvement of PiT1 in enamel mineralization, the underlying mechanisms are unknown (Yoshioka et al., 2011). Finally, a comprehensive study reported a strong expression of PiT2 in pulp cells, a fainter expression in ameloblasts and an absence of expression in odontoblasts at all stages of development (Zhao et al., 2006). In summary, despite the considerable need of Pi for tooth mineralization, knowledge on the mechanisms and molecules involved in the production and regulation of the Pi flux to the sites of mineral formation by the mineralizing cells are very scarce.

As a first step to determine the functional involvement of Pi transporters in tooth mineralization, the objective of this study was to characterize the expression of the six known Pi transporters in ameloblast-ALC (Nakata et al., 2003) and odontoblast-M2H4 (Ritchie et al., 2002) cell lines. To this aim, we used the ALC mouse ameloblast-lineage (Nakata et al., 2003) and in the M2H4 rat odontoblast (Ritchie et al., 2002) cell lines after optimization of the culture conditions necessary to ob-

tain a robust mineralization.

Material and Methods

Cell culture and conditions

The odontoblastic rat M2H4 cells, cloned from the rat dental pulp cell line RPC-C2A, were cultured as previously described (Magne et al., 2004), in a maintenance medium consisting of MEM (Minimal Essential Medium, Invitrogen 21090-022) containing 10% fetal bovine serum (FBS, Pan Biotech GmbH), 1% penicillin/streptomycin (Invitrogen) and 1% L-glutamine (Invitrogen). Cells were subcultured once a week using trypsin/EDTA, and maintained at 37 °C in a humidified atmosphere of 5% CO2 in air. To induce odontoblast differentiation, MEM was switched to α -MEM (Invitrogen 22571-020) containing ascorbic acid. To induce extracellular matrix mineralization, 3 mM inorganic phosphate (Pi) were added to the culture medium on day 2. Pi was added as a mixture of NaH2PO4 and Na2HPO4 (pH 7.3).

The immortalized mouse ameloblast-lineage cells (ALC) (generously provided by Dr. Toshihiro Sugiyama, Akita University, Japan) were seeded at a density of 10,000 cells/cm² and maintained at 37°C in a humidified atmosphere of 5% CO2 in air. The ALC were cultured in high-glucose Dulbecco’s modified Eagle’s medium (High Glucose Glutamax DMEM, Invitrogen 31966-021) supplemented with 10% FCS, 1% penicillin/streptomycin and 10ng/mL rhEGF (recombinant human Epidermal Growth Factor, R&D Systems) on collagen

I -coated (Rat Tail collagen I solution, BD Bioscience USA) culture plates, as described previously (Nakata et al., 2003; Takahashi et al., 2007). The growth medium was changed every 2 days. In order to induce mineralization, other media were evaluated including betaglycerophosphate (BGP, Sigma Aldrich G6251), ascorbic acid (Sigma Aldrich A4034), ITS (insulin transferrin selenite, Sigma Aldrich) and dexamethasone (Sigma Aldrich).

RNA isolation and real time qPCR

Total RNA was extracted from M2H4 and ALC cells using a Nucleospin® RNA II kit (Macherey-Nagel, Germany) in accordance with the manufacturer’s instructions. After DNaseI treatment, the RNA was quantified using a UV spectrophotometer (Nanodrop ND-1000, Labtech, Palaiseau, France).

Real-time PCR was performed on a Bio-Rad CFX96 using SYBR®Select Master Mix (Life Technologies). The following temperature profile was used: initial denaturation at 95°C for 3 minutes, followed by 40 cycles of 5 seconds at 95°C and 20 seconds at 60°C. Expression of target genes were normalized to GusB or GAPDH expression levels and the 2- $\Delta\Delta$ Ct (cycle threshold) method was used to calculate relative expression levels as previously described (Livak et al., 2001). The sequences of primers used in this study are listed in the Table 1.

Alizarin Red Staining

Calcium deposition in M2H4 and ALC cells culture was detected using Alizarin Red staining as previously described (Magne et al., 2004). Briefly, the extracellular matrix was

| Gene | Mouse | |
|--------|------------------------|------------------------|
| | Sense (5’-3’) | Antisense (5’-3’) |
| GusB | CTCTGGTGGCCTTACCTGAT | CAGTTGTTGTACCTTCACCTC |
| GAPDH | | |
| Npt1 | TCCTGGAAGAAGGAAGGGCCGT | CAGGGAAGGACCCCAAAGCCC |
| Npt2a | AGCCCCAGGGAGAAGCTATC | CCACAGTAGGATGCCCGAGA |
| Npt2b | CAGGACACTGGGATCAAATGG | GAAGGCGCTGCTCAGTACATC |
| Npt2c | CAGCCCTGCAGACATGTTAAT | GCACCAGGTACCACAGCAG |
| PiT1 | TGTGGCAAATGGGCAGAAG | AGAAAGCAGCGGAGAGACGA |
| PiT2 | CCATCGGCTTCTCACTCGT | AAACCAGGAGGCGACAATCT |
| DMP1 | | |
| COL1A1 | | |
| AMELX | TTCAGCCTCATCACCACTT | AGGGATGTTTGGCTGATGGT |
| TUFT1 | ACTGTGCAGGAGTTGCTTGTC | ATTTCTGCCGCTTTCTGCTCCA |

| Gene | Rat | |
|--------|--------------------------|-----------------------|
| | Sense (5'–3') | Antisense (5'–3') |
| GusB | | |
| GAPDH | GAGCCAAACGGGTCATCA | CATATTTCTCGTGGTTCACCC |
| Npt1 | TCCTGGAAGAAGGAAGGGCCGT | CAGGGAAGGACCCCAAAGCCC |
| Npt2a | TCACAGTCTCATTTCGGATTTGGT | GCAGCCCAGTATCCACGAAGA |
| Npt2b | TGCTAACATCGGGACCTCCA | AGCTCCTGCAAATGCCCTTC |
| Npt2c | GCACCACCACCACAGCCTTAC | GCCAGCCAGGTTGAAAAAGAA |
| PiT1 | GGAAGGACCTGACACCAATC | GGGAAGGCCAATGTTTTGAT |
| PiT2 | CCATCGGCTTCTCACTCGT | AAACCAGGAGGCGACAATCT |
| DMP1 | TTTGACCCAGTCGGAAGAGA | CATATTGGGATGCGATTTCCT |
| COL1A1 | CATGTTTCAGCTTTGTGGACCT | GCAGCTGACTTCAGGGATGT |
| AMELX | | |
| TUFT1 | | |

Sequence of primers for RT-PCR

washed with cold PBS and stained with 2% Alizarin Red solution for 2 minutes. Stained cells were extensively washed with deionized water to remove any nonspecific staining. Photographs were obtained with a light microscope (Leica DFC 450C®). Alizarin Red was extracted using a solution of 20% methanol and 10% acetic acid in water. After 15 minutes, the liquid was harvested and the Alizarin Red optical density was determined on a spectrophotometer (Victor3 1420 Multilabel Counter®) using a wavelength of 450 nm.

Statistical analysis

Experiments were repeated at least three times. Depending on the number of samples and their distribution, results were analysed using a one-way ANOVA, unpaired Student's t test or a non-parametric Mann and Witney test. A p-value < 0.05 was considered statistically significant. When not specified on figures, results were considered as not significant.

Results

ALC mineralization culture conditions optimization

ALC were described to form few calcified nodules at day 14 to 21 (Nakata et al., 2003; Takahashi et al., 2007) in medium 1 (see Table 2). In order to induce an earlier and stronger matrix mineralization, we compared 9 different culture conditions, based on known *in vitro* mineralization conditions. The most intense Red Alizarin staining was obtained with media 4 and 5 after 10 and 18 days following mineralization induction at day 2 (Figure 1).

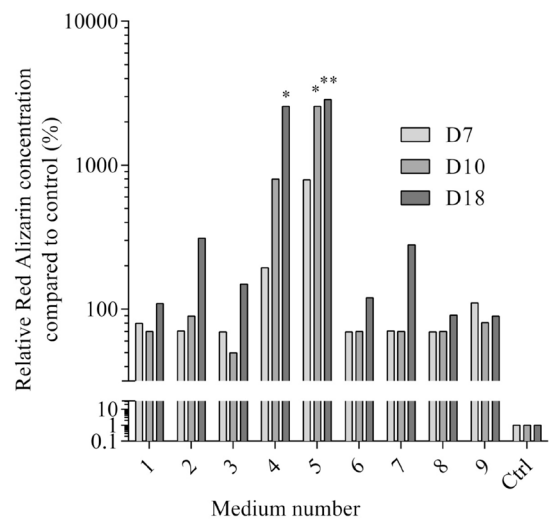


Figure 1: ALC mineralization in vitro obtained in different media.

ALC were seeded at day 0 (D0) in Medium 1 (Table 1) at 10,000cells/cm². At day 2 (D2) when cells were subconfluent, growth medium was switched to a mineralization medium (Media 2-8). After mineralization induction, cells were stained with Alizarin Red S at different times: 7 days (D7), 10 days (D10) and 18 days (D18) post induction; and absorbance of the Alizarin Red S extract solution was measured at 405nm. Each absorbance result was compared to medium 1 result of the same day * p<0.05 and ** p<0.01 (not specified=not significant).

Medium 5 is identical to medium 4 with the exception that 4mM BGP was used instead of 2mM. Medium 5 allowed a higher mineralization rate, with a reduced delay of induction than in medium 4 and original medium 1 (Figure 1). A significant Red Alizarin staining

| | |
|------------|--|
| Medium 1 : | DMEM Glutamax High Glucose + 10% FCS + 1% penicillin/streptomycin + 10ng/mL rhEGF |
| Medium 2 : | Medium 1 + 2mM beta-glycerophosphate (BGP) + 50µg/mL ascorbic acid |
| Medium 3 : | Medium 2 + 1µg/mL Insulin Transferrin Selenite (ITS) |
| Medium 4 : | Medium 2 + 10 ⁻⁸ M dexamethasone |
| Medium 5: | Medium 1 + 4mM beta-glycerophosphate (BGP) + 50µg/mL ascorbic acid+ 10 ⁻⁸ M dexamethasone |
| Medium 6 : | alpha-MEM + 10% FCS + 2mM BGP + 50µg/mL ascorbic acid + 1% penicillin/streptomycin + 10ng/mL rhEGF |
| Medium 7 : | Medium 6 + 1ug/mL ITS |
| Medium 8 : | Medium 7 + 10 ⁻⁸ M de dexamethasone |
| Medium 9 : | Medium 1 on a 300µm ivory cut |

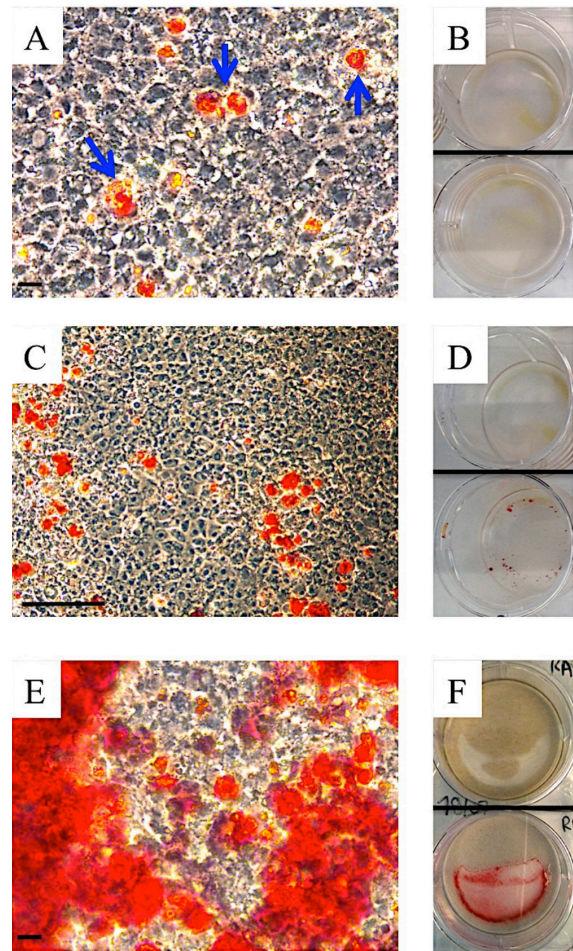
Culture conditions used for ALC mineralization induction.

was obtained after only 4 days (D4) in medium 5. At D7, wells cultured with media 4 and 5 showed many calcification nodules (Figure 2A-B), which grew until covering the cell layer (Figure 2C-H). Cells shape and number were similar in media 1 and 5, with no statistically difference neither in metabolic activity nor cell viability (MTT assays, data not shown). Therefore, we chose medium 5 for further investigations on ALC mineralization in vitro.

Phosphate transporters expression in ALC in vitro

After 7 and 25 days of culture, the phosphate transporters Npt1, Npt2a and Npt2c expressions were undetectable in mineralization media, as well as in proliferation medium (data not shown). At day 7 of culture, only PiT1 and PiT2 were expressed in ALC cultured in both media, with PiT1 mRNA being more abundant than PiT2 (Figure 3). At day 25 of culture, PiT1 and PiT2 were expressed in ALC cultured in both media. Npt2b was expressed only in ALC cultured in the mineralization-inducing medium, at D7, but at a very low level compared to PiT1 and PiT2. PiT1 and PiT2 showed the highest mRNA expression in ALC culture in both media (Figure 3).

To further study the expression of PiT1 and PiT2 in ALC, we monitored their expression in a proliferation (medium 1) or mineralization (medium 5) medium over time (Figure 4). Both PiT1 and PiT2 expressions increased slowly and moderately in medium 1 up until 29 days



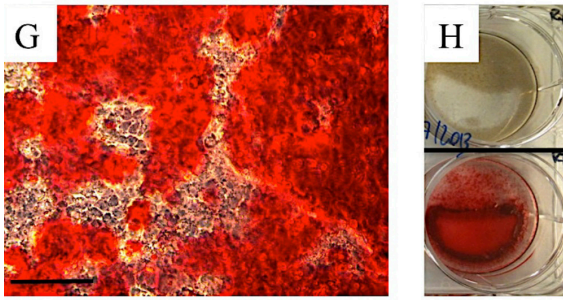


Figure 2: ALC mineralization cultured in medium 5 ALC were seeded at day 0 in Medium 1 (Table 1) at 10,000cells/cm². At day 2 when cells were sub confluent, growth medium was switched to the mineralization medium 5. After mineralization induction, cells were stained with Alizarin Red S at different times: 4 days (A&B) 7 days (C&D), 10 days (E&F) and 18 days (G&H) of culture. Calcification nodules are stained in red (blue arrows). Cells in the well up the line were cultured in medium 1 (control), cells in the well down the line in medium 5, then stained with Red Alizarin (B, D, F H).

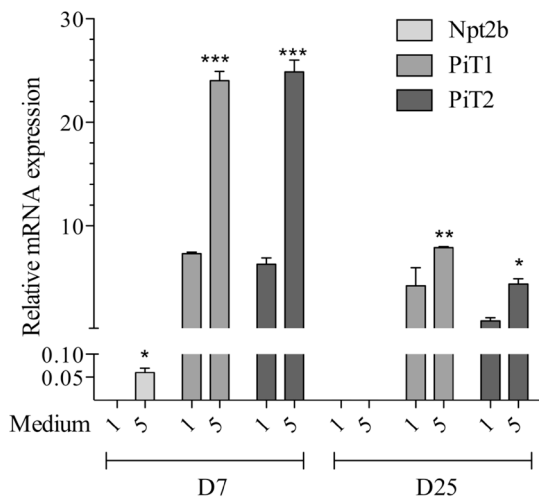


Figure 3: Comparative mRNA expression of the phosphate transporters at 7 and 25 days of culture in a growth medium or in mineralization-inducing medium by ameloblast-lineage cells (ALC).

ALC were seeded at day 0 in Medium 1 (Table 1) at 10,000cells/cm². At day 2 when cells were sub confluent, growth medium 1 was switched or not to the mineralization medium 5. Culture was stopped after 7 days (D7) and 25 days (D25) of culture, and mRNA was extracted.

At each time, values of medium 1 and medium 5 were compared with * p<0.05, ** p<0.01 and *** p<0.005 (not specified=not significant)

of culture. In medium 5, the expression of the transporters was much higher than in medium 1 and peaked at 14 days of culture (Figure 4). Importantly, this latter expression profile did not correlate with the mineralization kinetics (Figure 2).

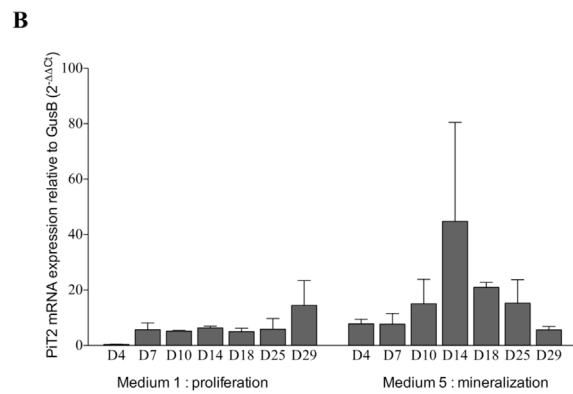
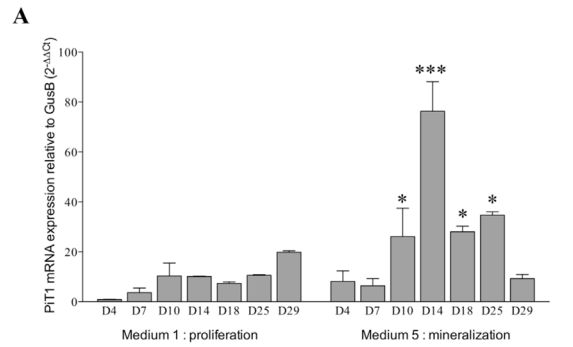


Figure 4: Relative mRNA expression of PiT1 and PiT2 in ameloblast-lineage cells (ALC) culture with or without mineralization induction in long-term culture.

ALC were seeded at day 0 in Medium 1 (Table 1) at 10,000cells/cm². At day 2 when cells were sub confluent, proliferation medium 1 was switched or not to the mineralization medium 5. Culture was stopped after 4 days (D4) to 29 days (D29) of culture, and mRNA was extracted. PiT1 (A) and PiT2 (B) mRNA expressions were compared to GusB expression (2^{-ΔΔCt}). At each time, values of medium 1 and medium 5 were compared with * p<0.05 *** p<0.001 (not specified=not significant).

Ameloblastic hallmarks in ALC culture

As previously described, ALC expressed amelogenin (AmelX) and tuftelin (Tuft1), two of the ameloblast-phenotype hallmark genes (Nakata et al., 2003). Both amelogenin (Figure 5.A) and tuftelin (Figure 5.B) expressions softly increased in medium 1. When cultured in medium 5, their expressions peaked at 14 days of culture. Tuftelin, amelogenin, PiT1 and PiT2 kinetics of expression were very alike, although our results could not demonstrate a strong correlation between ameloblastic marker expression and ALC mineralization kinetics (Figures 2-4-5). The level of enamel expression was globally too low to be reliable, but exhibited a faint expression starting at 25 days of culture (data not shown).

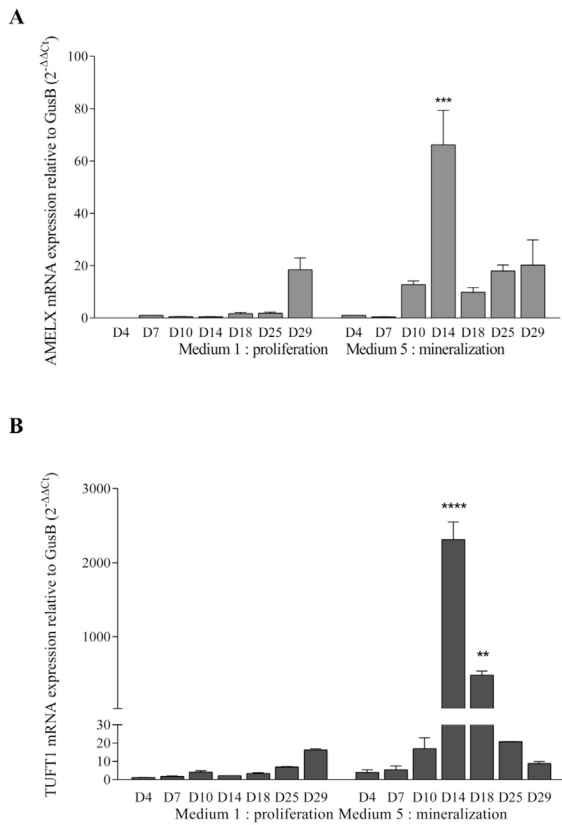


Figure 5: Relative mRNA expressions of ameloblastic hallmarks in ameloblast-lineage cells (ALC) culture with or without mineralization induction in long-term culture. ALC were seeded at day 0 in Medium 1 (Table 1) at 10,000 cells/cm². At day 2 when cells were sub confluent, proliferation medium 1 was switched or not to the mineralization medium 5. Culture was stopped after 4 days (D4) to 29 days (D29) of culture, and mRNA was extracted. Tuftelin TUFT1 (A) and amelogenin AMELX (B) mRNA expressions were compared to GusB expression (2^{-ΔΔCt}). ENAM (enamelin) mRNA levels were too low to be reliable. At each time, values of medium 1 and medium 5 were compared with ** p<0.005 *** p<0.001 **** p<0.0005 (not specified=not significant)

M2H4 odontoblast mineralization in vitro

Specific Ca nodules when M2H4 were cultured in mineralization medium were obtained only 24h after the medium switch, even though this mineralization became statistically significant only after 48h (Figures 6 and 7). After 7 days in mineralization culture conditions, the culture well was entirely covered by specific calcifications colored by intense Red Alizarin staining (Figure 6). There was no calcification in the control condition (MEM alone). These results confirmed previous results obtained by Magne et al. (2004) using M2H4 cells.

Expression of phosphate transporters and odontoblast hallmarks in M2H4 cells

PiT1 and PiT2 were highly expressed compa-

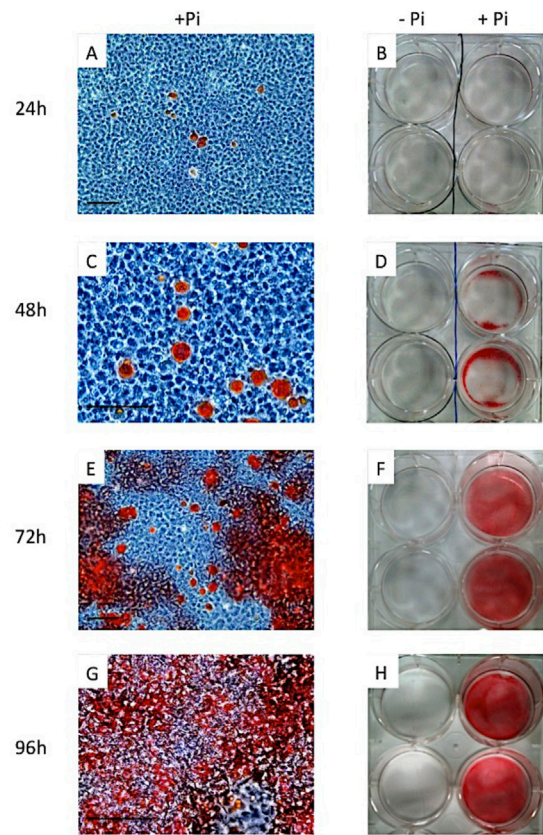


Figure 6: M2H4 mineralization in culture M2H4 were cultured in the maintenance medium without phosphate (-Pi) and seeded at 10,000 cells/cm² at day 0. To induce odontoblast differentiation and mineralization, MEM was switched to α-MEM with phosphate (+Pi) when cells were subconfluent at day 2. Alizarin Red staining revealed specific Ca nodules from 24h after induction, without any aspecific staining in control (- Pi). A-B: 24 hours after induction. C-D: 48 hours after induction. E-F: 72 hours after induction. G-H: 96 hours after induction.

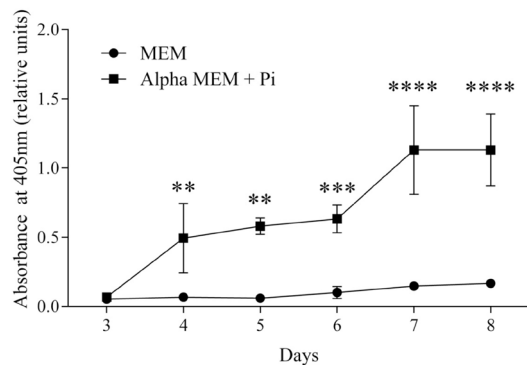


Figure 7: M2H4 mineralization kinetics M2H4 were seeded at D0 in MEM at 10,000 cells/cm². At D2 when cells were subconfluent, in order to induce odontoblast differentiation and mineralization, MEM was switched to α-MEM+Pi. Wells were stained with Alizarin Red at day 3-4-5-6-7-8 and absorbance of the Red Alizarin extract was measured by spectrophotometry at 450 nm. At each time, values of MEM and alpha MEM + Pi were compared with ** p<0.005 *** p<0.001 **** p<0.0005 (not specified=not significant)

red to the other phosphate transporters Npt1, Npt2a, Npt2b and Npt2c for which no expression could be detected in this cell line. No difference in PiT expressions could be seen between the mineralization and proliferation medium (Figure 8). During cell culture period, the expression of PiT1 and PiT2 decreased, whereas as described above, cell mineralization increased. M2H4 were found to express

two of the specific odontoblast-phenotype hallmarks previously described (Magne et al., 2004), DMP1 (dentin matrix protein 1) and COL1A1 (collagen type I), with strong mRNA levels in both mineralization and proliferation media (Figure 9). DMP1 expression increased with time and reached a maximum at day 5-6 (Figure 9.A). COL1A1 expression was almost constant during the culture period, without any clear difference between the two media (Figure 9.B).

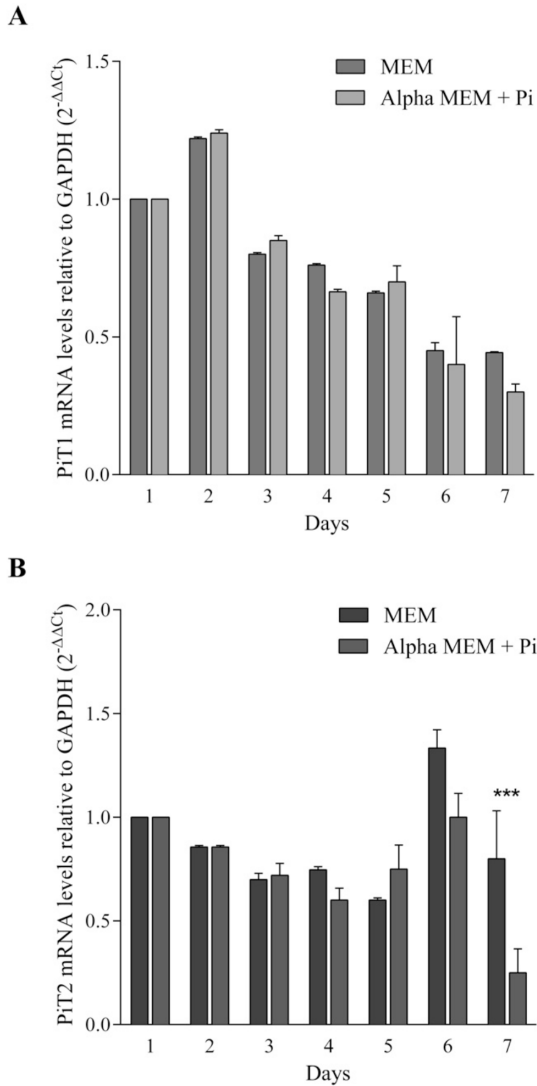


Figure 8: Relative mRNA expressions of PiT1 and PiT2 in odontoblast cells (M2H4) culture with or without mineralization induction.

M2H4 were seeded at D0 in MEM at 10,000cells/cm². At D2 when cells were subconfluent, in order to induce odontoblast differentiation and mineralization, MEM was switched to α-MEM+Pi. Culture is stopped after 1 to 7 days of culture, and mRNA was extracted. PiT1 (A) and PiT2(B) mRNA expressions were compared to GAPDH expression (2^{-ΔΔCt}). At each time, values of MEM and alpha MEM + Pi were compared with *** p<0.001 (not specified=not significant)

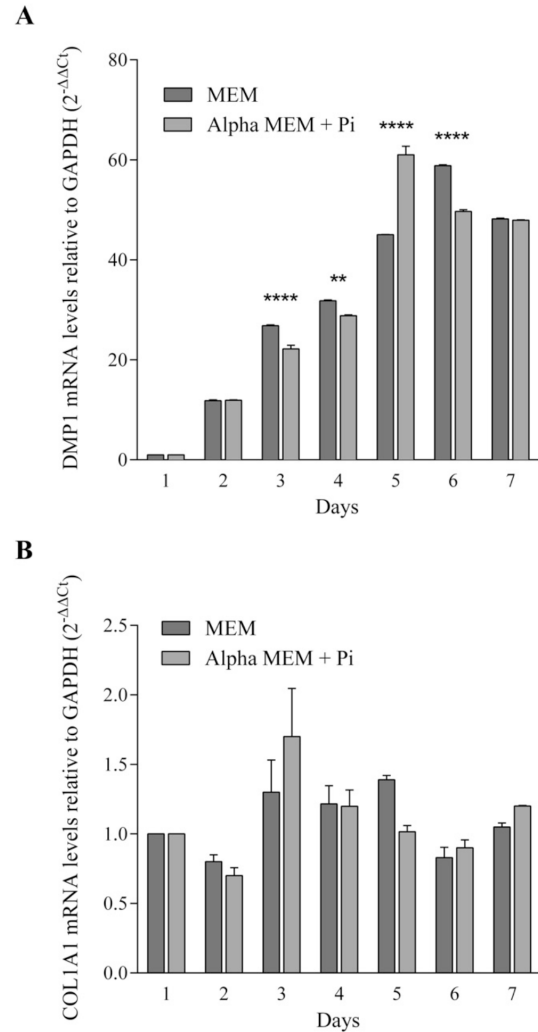


Figure 9: Relative mRNA expressions of odontoblastic hallmarks DMP1 (dentin matrix protein 1) and COL1A1 (collagen 1) in odontoblast cells culture with or without mineralization induction.

M2H4 were seeded at D0 in MEM at 10,000cells/cm². At D2 when cells were subconfluent, in order to induce odontoblast differentiation and mineralization, MEM was switched to α-MEM+Pi. Culture is stopped after 1 to 7 days of culture, and mRNA was extracted. DMP1 (A) and COL1A1 (B) mRNA expressions were compared to GAPDH expression (2^{-ΔΔCt}).

At each time, values of MEM and alpha MEM + Pi were compared with ** p<0.005 and **** p<0.0005 (not specified=not significant)

Discussion

Transport of Pi and calcium ions through the dental tissues is essential for the formation of dentin and enamel, the most highly mineralized tissues in the mammalian body. Although the underlying mechanisms and factors governing calcium transport in odontogenesis have been elucidated to some extent (Hubbard, 2000), the characteristics and regulation of Pi transport in dental tissues remain largely unknown.

In this study, we chose two dental cells models, the mouse ameloblast lineage cell line ALC and the rat odontoblast cell line M2H4, to investigate the phosphate transporters involvement in enamel and dentin mineralization *in vitro*, respectively.

Even though mesenchymal cell lines can easily be differentiated into osteoblasts or chondrocytes, the possibilities for having mineralizing dental cell line models are scarce, especially for the ameloblast lineage. As for the odontoblast cell lineage, the development of a pulp cell line such as the rat RPC-C2A cell line (Kasugai et al., 1988) has enabled to derive odontoblast-like cell lines such as the MRPC-1 and M2H4 cells. These rat cell lines are known to express some dentin specific markers such as DMP1 or DSPP and to produce mineralized nodules. The mineralized matrix formed by M2H4 after Pi adjunction was characterized by FTIR and was shown to be equivalent to the one from rat dentin (Magne et al., 2004). These cells are not the only odontoblast cell lines available. The mouse odontoblastic MO6-G3 cell line derived from the transformed pulpal cell line HPC-T was generated for the evaluation of gene expression by MacDougall et al. (1995), and a porcine pulp derived odontoblast cell line expressing dentin specific hallmarks was also a possible choice for dentin mineralization investigations (Iwata et al., 2007). As for enamel mineralization, our choice was more limited as the ameloblast-cell lines available at the beginning of this study were the murine LS8 (Chen et al., 1992), porcine PABSo-E (Denbesten et al., 1999), rat HAT-7 (Kawano et al., 2002), and the murine ALC (Nakata et al., 2003) cells. Among these models, only the ALC were described to form few calcified nodules *in vitro* and a quite recent study comparing LS8 and ALC showed that ALC were a more suitable model to the study of enamel matrix mineralization processes as this cell line express more markers of maturation-stage events of amelo-

genesis (Sarkar J. et al., 2014). We showed in our study strong expression of specific ameloblastic hallmarks in both proliferation and mineralization media. The optimization of the ALC mineralization medium was conclusive as we obtained *in vitro* calcifications in ALC after only 4 days which increased over time. This medium is an "osteogenic like media", as it contains BGP, ascorbate and dexamethasone. BGP as a phosphate source is subjected to the alkaline phosphatase activity, which is expressed by ALC in our mineralizing conditions after 7 days of culture (data not shown), and it has been shown to be expressed by mature ameloblasts (Hotton et al., 1999). This study confirms that M2H4 (rat odontoblast) and ALC (mouse mature ameloblast) after culture conditions optimization are good mineralization dental cell lines models to study the involvement of phosphate transporters in tooth mineralization *in vitro*.

This study showed that the two phosphate transporters expressed *in vitro* in these two cell lines models are PiT1 and PiT2. No expression of the other phosphate transporters (Npt1, Npt2a, Npt2b and Npt2c) was detected by qPCR in these *in vitro* models. But Lundquist et al. (2002) showed by immunohistochemistry that Npt2a and Npt2b were expressed both in odontoblasts and ameloblasts in 10-day old mice, as well as they showed that these transporters were expressed in rat odontoblast MRPC-1 culture. Furthermore, Onishi et al. (2007) showed by *in situ* hybridization that Npt2b was expressed in mice at 2, 6 and 10 days after birth in odontoblasts and in both secretory and mature ameloblasts, and Lacruz et al. (2012) confirmed the potential role of Npt2b in ameloblast mineralization processes. This might be explained by the lack of ectomesenchymal interactions in our *in vitro* model, compared to the literature *in vivo* results. In our models, PiT1 and PiT2 are the only phosphate transporters strongly expressed, PiT2 in either proliferation or in mineralization culture conditions. These results are consistent with most *in vitro* results of the literature obtained in the mouse odontoblastic MO6-G3 cell line (Wittrant et al., 2009; Bourguine et al., 2011) and human pulp cells differentiated into odontoblasts (Tada et al., 2011). No work had been done in ameloblasts *in vitro* on phosphate transporters. However, these *in vitro* results are not fully consistent with previous *in vivo* results and not necessarily consistent with each other. Zhao et al. (2006)

described the ontogenesis of PiT2 in mouse odontogenesis and established that PiT2 was expressed in dental cells at various stages and different levels of expression but never in odontoblasts from 11,5 embryonic days to 14 days post natal. Conversely Yoshioka et al., (2011) showed amelogenesis impairment in a PiT1 over expression rat model. As the mineralization and expression of PiT1 and PiT2 kinetics are not correlated in this study, and for the heterogeneity of previous results, we can not therefore conclude on phosphate transporters implication in tooth mineralization without any *in vivo* functional and global investigations.

To this aim, further studies must be engaged to determine which phosphate transporters are implicated or not in dentin and enamel mineralization processes *in vivo*: ontogenesis of the six phosphate transporters during whole dental development by *in situ* hybridization and/or immunohistochemistry, and dental tissue specific invalidations of the phosphate transporters.

In conclusion, through the optimization of mineralization conditions of rat odontoblast and mouse ameloblasts cells, we showed that both PiT1 and PiT2 were highly expressed in these cells but that their expression did not correlated with the mineralization processes. Although a role of phosphate transporters in enamel and dentin mineralization processes can not be excluded, these results are not in favor of a functional implication of these molecules in the tooth mineralization processes.

Acknowledgments

This study was supported by an IFRO (Institut Français de la Recherche Odontologique) grant. We greatly thank Dr Toshihiro Sugiyama, Dr Akira Nakata and Dr Carolyn W. Gibson for providing the ALC cell line.

Bibliography

Beck, L., Karaplis, A.C., Amizuka, N., Hewson, A.S., Ozawa, H. and Tenenhouse, H.S., Targeted inactivation of Npt2 in mice leads to severe renal phosphate wasting, hypercalciuria, and skeletal abnormalities. Proc Natl Acad Sci U S A, 1998. 95(9): p. 5372-7.

Beck, L., Leroy, C., Beck-Cormier, S., Forand, A., Salaün, C., Paris, N., Bernier, A., Ure-

ña-Torres, P., Prié, D., Ollero, M., Coulombel, L. and Friedlander, G., The Phosphate Transporter PiT1 (Slc20a1) Revealed As a New Essential Gene for Mouse Liver Development. PLoS ONE, 2010. 5(2): p. e9148.

Beck, L., Leroy, C., Salaun, C., Margall-Ducos, G., Desdouets, C. and Friedlander, G., Identification of a novel function of PiT1 critical for cell proliferation and independent of its phosphate transport activity. J Biol-Chem, 2009. 284(45): p. 31363-74

Boskey A.L. and Roy R., Cell Culture Systems for Studies of Bone and Tooth Mineralization, Chem Rev. 2008 Nov; 108(11): p.4716–4733.

Bourgine, A., Beck, L., Khoshniat, S., Wauquier, F., Oliver, L., Hue, E., Alliot-Licht, B., Weiss, P., Guicheux, J. and Wittrant, Y., Inorganic phosphate stimulates apoptosis in murine MO6-G3 odontoblast-like cells. Arch Oral Biol, 2011. 56(10): p. 977-83.

Byskov, K., Jensen, N., Kongsfelt, I.B., Wielse, M., Pedersen, L.E., Haldrup, C. and Pedersen, L., Regulation of cell proliferation and cell density by the inorganic phosphate transporter PiT1. Cell Div, 2012. 7(1): p. 7.

Chen L. S., Couwenhoven D., Hsu D., Luo W., Snead M. L. Maintenance of amelogenin gene expression by transformed epithelial cells of mouse enamel organ. Arch. Oral Biol. 1992. 37, 771–778

Corut, A., Senyigit, A., Ugur, S.A., Altin, S., Ozcelik, U., Calisir, H., Yildirim, Z., Gocmen, A. and Tolun, A., Mutations in SL-C34A2 cause pulmonary alveolar microlithiasis and are possibly associated with testicular microlithiasis. Am J Hum Genet, 2006. 79(4): p. 650-6.

Gaucher C., Boukpepsi T., Septier D., Jehan F., Rowe P.S., Garabédian M., Goldberg M., Chaussain-Miller C., Dentin noncollagenous matrix proteins in familial hypophosphatemic rickets. Cells Tissues Organs. 2009;189(1-4): p. 219-23.

Denbesten P. K., Gao C., Li W., Mathews C. H., Gruenert D. C. Development and characterization of an SV40 immortalized por-

- cine ameloblast-like cell line. *Eur. J. Oral Sci.* 1999. 107, 276–281
- Forster IC1, Hernando N, Biber J, Murer H., Phosphate transporters of the SLC20 and SLC34 families. *Mol Aspects Med.*, 2013 Apr-Jun;34(2-3):386-95
- Goldberg, M., Kulkarni, A.B., Young, M. and Boskey, A., Dentin: structure, composition and mineralization. *FrontBiosci (Elite Ed)*, 2011. 3(3): p. 711-35.
- Goncalves P.F., Sallum E.A., Sallum A.W., Casati M.Z., de Toledo S. and Nociti Jr F.H., Dental cementum reviewed: development, structure, composition, regeneration and potential functions. *Braz J Oral Sci.* 4(12): 651-658
- Hotton D., Mauro N., Lézot F., Forest N., Bernal A. Differential expression and activity of tissue-nonspecific alkaline phosphatase (TNAP) in rat odontogenic cells in vivo. *J Histochem Cytochem.* 1999;47(12):1541-52.
- Hubbard MJ., Calcium transport across the dental enamel epithelium. *Crit Rev Oral Biol Med.* 2000; 11:437–466.
- Iharada M, Miyaji T, Fujimoto T, Hiasa M, Anzai N, Omote H, Moriyama Y., Type 1 sodium-dependent phosphate transporter (SLC17A1 Protein) is a Cl(-)-dependent urate exporter. *J Biol Chem.* 2010 Aug 20;285(34):26107-13.
- Iwata T, Yamakoshi Y, Simmer JP, Ishikawa I, Hu JC., Establishment of porcine pulp-derived cell lines and expression of recombinant dentin sialoprotein and recombinant dentin matrix protein-1., *Eur J Oral Sci.* 2007 Feb;115(1):48-56.
- Kawano S., Morotomi T., Toyono T., Nakamura N., Uchida T., Ohishi M., Toyoshima K., Harada H. Establishment of dental epithelial cell line (HAT-7) and the cell differentiation dependent on Notch signaling pathway. *Connect. Tissue Res.* 2002. 43, 409–412
- Kasugai S1, Adachi M, Ogura H., Establishment and characterization of a clonal cell line (RPC-C2A) from dental pulp of the rat incisor., *Arch Oral Biol.* 1988;33(12):887-91.
- Khoshniat, S., Bourguine, A., Julien, M., Weiss, P., Guicheux, J. and Beck, L., The emergence of phosphate as a specific signaling molecule in bone and other cell types in mammals. *Cell. Mol. Life Sci.*, 2010. 68(2): p. 205-218.
- Lacruz RS, Smith CE, Kurtz I, Hubbard MJ, Paine ML., New paradigms on the transport functions of maturation-stage ameloblasts, *J Dent Res.* 2013 Feb;92(2):122-9.
- Livak, K. and Schmittgen, T., Analysis of relative gene expression data using real-time quantitative PCR and the 2(-Delta Delta C(T)) Method. *Methods.* 2001. 25(4): p. 402-8.
- Lundquist, P., Odontoblast phosphate and calcium transport in dentinogenesis. *Swed Dent J Suppl*, 2002. Supplement 154(154): p. 1-52.
- Lundquist, P., Ritchie, H.H., Moore, K., Lundgren, T. and Linde, A., Phosphate and calcium uptake by rat odontoblast-like MRPC-1 cells concomitant with mineralization. *J. Bone Miner. Res.*, 2002. 17(10): p. 1801-1813.
- MacDougall M1, Thiemann F, Ta H, Hsu P, Chen LS, Snead ML., Temperature sensitive simian virus 40 large T antigen immortalization of murine odontoblast cell cultures: establishment of clonal odontoblast cell line., *Connect Tissue Res.* 1995;33(1-3):97-103.
- Magne, D., Bluteau, G., Lopez-Cazaux, S., Weiss, P., Pilet, P., Ritchie, H.H., Daculsi, G. and Guicheux, J., Development of an odontoblast in vitro model to study dentin mineralization. *Connect Tissue Res*, 2004. 45(2): p. 101-108.
- Miyamoto, K., Haito-Sugino, S., Kuwahara, S., Ohi, A., Nomura, K., Ito, M., Kuwahata, M., Kido, S., Tatsumi, S., Kaneko, I. and Segawa, H., Sodium-dependent phosphate cotransporters: lessons from gene knockout and mutation studies. *J Pharm Sci*, 2011. 100(9): p. 3719-30.
- Onishi, T., Okawa, R., Ogawa, T., Shintani,

- S. and Ooshima, T., Phex mutation causes the reduction of npt2b mRNA in teeth. *Journal of Dental Research*, 2007. 86(2): p. 158-162.
- Opsahl Vital, S., Gaucher, C., Bardet, C., Rowe, P.S., George, A., Linglart, A. and Chaussain, C., Tooth dentin defects reflect genetic disorders affecting bone mineralization. *Bone*, 2012. 50(4): p. 989-97.
- Palmer, G., Zhao, J., Bonjour, J., Hofstetter, W. and Caverzasio, J., In vivo expression of transcripts encoding the Glvr-1 phosphate transporter/retrovirus receptor during bone development. *Bone*, 1999. 24(1): p. 1-7.
- Ritchie, H.H., Liu, J., Kasugai, S. and Moller, P., A mineralizing rat dental pulp cell subline expressing collagen type I and dentin sialoprotein-phosphophoryn transcripts. *In Vitro Cell Dev Biol Anim*, 2002. 38(1): p. 25-9.
- Sabbagh, Y., O'Brien, S.P., Song, W., Boulanger, J.H., Stockmann, A., Arbeeny, C. and Schiavi, S.C., Intestinal npt2b plays a major role in phosphate absorption and homeostasis. *J Am Soc Nephrol*, 2009. 20(11): p. 2348-58.
- Salaun, C., Leroy, C., Rousseau, A., Boitez, V., Beck, L. and Friedlander, G., Identification of a novel transport-independent function of PIT1/SLC20A1 in the regulation of TNF-induced apoptosis. *J Biol Chem*, 2010. 285(45): p. 34408-18.
- Sarkar J., Simanian EJ.,Tuggy SY., Bartlett JD., Snead ML., Sugiyama T., Paine ML. Comparison of two mouse ameloblast-like cell lines for enamel-specific gene expression. *Front Physiol*. 2014; 5:277.
- Segawa, H., Onitsuka, A., Furutani, J., Kaneko, I., Aranami, F., Matsumoto, N., Tomoe, Y., Kuwahata, M., Ito, M., Matsumoto, M., Li, M., Amizuka, N. and Miyamoto, K.i., Npt2a and Npt2c in mice play distinct and synergistic roles in inorganic phosphate metabolism and skeletal development. *AJP: Renal Physiology*, 2009. 297(3): p. 671-678.
- Tada, H., Nemoto, E., Foster, B.L., Somerman, M.J. and Shimauchi, H., Phosphate increases bone morphogenetic protein-2 expression through cAMP-dependent protein kinase and ERK1/2 pathways in human dental pulp cells. *Bone*, 2011. 48(6): p. 1409-1416.
- Veis, A. and Dorvee JR., Biomineralization mechanisms: a new paradigm for crystal nucleation in organic matrices. *Calcif Tissue Int.*, 2013. 93(4):307-315.
- Villa-Bellosta, R., Ravera, S., Sorribas, V., Stange, G., Levi, M., Murer, H., Biber, J. and Forster, I.C., The Na⁺-Pi cotransporter PIT-2 (SLC20A2) is expressed in the apical membrane of rat renal proximal tubules and regulated by dietary Pi. *AJP: Renal Physiology*, 2009. 296(4): p. 691-699.
- Wagner CA1, Hernando N, Forster IC, Biber J., The SLC34 family of sodium-dependent phosphate transporters. *Pflugers Arch*. 2014 Jan;466(1):139-53
- Wittrant, Y., Bourguine, A., Khoshniat, S., Alliot-Licht, B., Masson, M., Gatius, M., Rouillon, T., Weiss, P., Beck, L. and Guicheux, J., Inorganic phosphate regulates Glvr-1 and -2 expression: role of calcium and ERK1/2. *Biochemical and Biophysical Research Communications*, 2009. 381(2): p. 259-263.
- Yoshioka, H., Yoshiko, Y., Minamizaki, T., Suzuki, S., Koma, Y., Nobukiyo, A., Sotomaru, Y., Suzuki, A., Itoh, M. and Maeda, N., Incisor Enamel Formation is Impaired in Transgenic Rats Overexpressing the Type III NaPi Transporter Slc20a1. *Calcif Tissue Int*, 2011. 89(3): p. 192-202.
- Zhao, D., VaziriSani, F., Nilsson, J., Rodenburg, M., Stocking, C., Linde, A. and Gritli-Linde, A., Expression of Pit2 sodium-phosphate cotransporter during murine odontogenesis is developmentally regulated. *Eur. J. Oral Sci.*, 2006. 114(6): p. 517-523.